Estuaries and Coasts (2026) 49:175
https://doi.org/10.1007/s12237-026-01759-6

Behavioral Response of Oyster Valve Gape to Ecological Conditions in an Intermittently Closed Estuary

Niv Anidjar[1] · Sarah N. Giddings[1] · Carlos Neira[1] · George Sugihara[1] · Lisa A. Levin[1] · Kristen A. Goodrich[3] · Jeff Crooks[3] · Duncan Wheeler[4] · Lillian R. McCormick[1,5] · Luke P. Miller[2]

Received: 29 August 2025 / Revised: 12 June 2026 / Accepted: 14 June 2026

Abstract

Low-inflow estuaries are highly variable and productive habitats. Organisms in these systems must cope with constantly changing conditions. This study investigates the continuous response of oysters to environmental stimuli in a small, low-inflow, estuary, Los Peñasquitos Lagoon (LPL), in San Diego, California, USA. The oysters were placed on a mooring at near-surface and near-bottom locations and instrumented with noninvasive sensors to measure their shell opening (oyster valve gape), concurrently with physical and chemical measurements (water depth, salinity, temperature, dissolved oxygen, pH, solar radiation, wind velocity, and wave radiation stresses) over 136 days. The time series of each oyster with each variable over tidally averaged and shorter time scales were analyzed using traditional statistical methods. The strongest gape relationships were with salinity and dissolved oxygen (Spearman correlation coefficient 0.6), among the oysters near the water surface. Diurnal phase averaging showed how the surface oysters open and close in phase with insolation, while the near-bottom oysters have a lagged response. Tidal phase averaging further illustrates the distinct gape behavior, with surface oysters closing consistently during low tides, and bottom oysters generally remaining open. A subset of variables that had high Spearman correlations (near surface oxygen and salinity, near-bottom pH, solar irradiance, and near-bottom turbidity) and their 18-hour time lags were used to test a set of multivariate models for predicting surface oyster valve gape. The best performing model ($r^2 = 0.75$) was consistent with the correlation analysis, showing salinity and dissolved oxygen to be the most important predictors. Key insights from this study are that oysters in LPL have predictable responses to environmental conditions (particularly salinity and dissolved oxygen) with differing responses to conditions near-surface and near-bottom on tidal and tidally-averaged, and faster than tidal timescales.

Keywords Low-inflow estuaries · Intermittently closed estuaries · *Crassostrea gigas* · Oyster valve behavior · Biological monitoring

Introduction

Estuaries have consistently been cited as one of the most economically valuable ecosystems (Costanza et al., 1997, 2014; de Groot et al., 2012). In the United States, eight of the ten largest metropolitan areas are in regions bordering estuaries, comprising 40% of the nation's population (Rouleau et al., 2021). Estuaries are sensitive to changes in climate which alter forcing from the atmosphere, ocean and upstream end members, while at the same time are subjected to significant direct human modifications. In order to mitigate the negative effects of human modifications, significant management and restoration projects have been implemented in impacted estuaries (Fuentes et al., 2020; Kennish, 2004; Walker et al., 2025). Monitoring estuarine conditions

Communicated by Eric N. Powell

✉ Niv Anidjar
nanidjar@ucsd.edu

1 Scripps Institution of Oceanography, UC San Diego, La Jolla, CA, USA

2 Coastal and Marine Institute, San Diego State University, San Diego, CA, USA

3 Tijuana River National Estuarine Research Reserve, San Diego, CA, USA

4 Tufts University, Medford, MA, USA

5 Bay-Delta Office, U.S. Bureau of Reclamation, Sacramento, CA, USA

Published online: 01 August 2026

in a cost effective and accessible manner is necessary for making such management decisions and implementing successful restoration plans (Roegner et al., 2008).

Low-Inflow estuaries (LIEs) are estuaries with minimal or intermittent freshwater input that exist worldwide in Mediterranean climates (Largier, 2023). Many of these LIEs experience a wide range in environmental and water quality conditions due to multiple compounding factors including the potential for hypersaline conditions and inverse or weak circulation (Largier, 2023). Many also experience significant mouth morphological changes including intermittent inlet mouth closure (intermittently closed estuaries, ICEs) during times of high waves and low freshwater flow (Behrens et al., 2013; McSweeney et al., 2017; Orescanin & Scooler, 2018). During times of weak or no circulation, poor water quality, including build up of pollution and development of hypoxia can occur (Cousins et al., 2010; Gale et al., 2007; Harvey et al., 2023).

Southern California LIEs and ICEs face a multitude of stressors and are heavily managed to avoid negative human and ecosystem consequences (for example, hypoxia, flooding, and mosquito breeding during inlet closures) (e.g., Elwany 2011). The patchwork of entities operating at different scales (e.g., local, state, regional, and federal), combined with divergent management objectives (e.g., ecological protection versus infrastructure maintenance), monitoring systems, and sensor networks, complicates the management landscape (Pratt, 2014; Sandag, 2025). Regional environmental managers have expressed a need to better understand when water quality conditions pose direct risks to biotic communities. In this context, biosentinels offer the potential to augment existing monitoring data and strengthen estuary management decision-making across these systems (Southern California Wetlands Recovery Project, 2018; Walker et al., 2025).

Often, environmental management bodies deduce biological dynamics from physical measurements and sparse biochemical measurements that involve slow benchtop analyses or single-use tests. Chemical water quality analysis can be expensive. Bae and Park (2014) note that the average cost to analyze 126 US EPA pollutants is $1000 per sample, and monitoring ecosystems at population and community levels can be slow (e.g., counting individuals). Comprehensive chemical analysis of all potential environmental toxins is not always possible (Bub et al., 2025). However, living organisms respond to a range of chemical and physical stimuli, through changes in behavior and physiological processes to maintain homeostasis. By measuring and describing behavioral and physiological variability, we can diagnose unusual behavior indicative of a change in the environment, possibly undetected by conventional sensors, or indicative of multi-stressors. Oysters are one organism that can act as these 'biological early warning systems' (BEWS) where patterns in their behavior (e.g., valve gape) reflect their health, possible stress, and response to their environment. BEWS have been used around the world (e.g., France, Germany, USA, China, Japan, and Korea) to monitor water quality through the behavior of individual organisms. BEWS have involved observing bacterial growth, algal fluorescence, plankton movements (e.g., *Daphnia*), fish movements, and bivalve behavior (Bae & Park, 2014). Sessile bivalves such as oysters are well suited as the basis for BEWS, due to their sensitivity to and bioaccumulation of contaminants, as well as their easy manageability in comparison with mobile organisms (Vereycken & Aldridge, 2023). Bivalves have been used to monitor water quality at least since the early 20th century with the work of Marceau (1909), and have been used for monitoring drinking water supplies in some locations (Borcherding, 2006; de Zwart et al., 1995). Bivalves are known to respond with their valve gape behavior to a broad set of environmental chemical changes including salinity, dissolved oxygen (DO), pH, copper, uranium, and toxic algae (Fournier et al., 2004; Porter & Breitburg, 2016; Tran et al., 2004, 2007, 2010).

The goal of this study is to investigate the continuous response of oyster valve gape to environmental stimuli in a small, low inflow, intermittently closed estuary subject to a wide range of conditions, providing baseline data for oyster valve response in an LIE and ICE. The study site is Los Peñasquitos Lagoon (LPL), a LIE and ICE located in San Diego, California, USA. Using an open source hardware and software system described in Miller (2022), *Crassostrea [Magallana] gigas* oysters in LPL were instrumented with noninvasive sensors to measure their shell opening (oyster valve gape) over time, concurrently with physical and biogeochemical measurements. The oyster monitors, as well as salinity, temperature, depth, and DO sensors were attached to a mooring in the LPL main channel, at two different depths (see Fig. 1). This vertical resolution allows for a deeper level of analysis not just of the oysters, but of their responses to stratification, which is an essential and well-studied component of estuarine dynamics. The study examined conditional averaging of oyster valve gape over diurnal, tidal, and spring/neap cycles, correlation of the time series of each oyster with each variable at tidally averaged and shorter time scales, and variable joint distributions. Given the relationships found between different environmental variables and nonlinear dynamics observed, we show the potential use of a multivariate function of environmental variables to predict oyster activity.

Compared with previous research involving oyster valvometry in estuaries, this work is a specialized effort at unifying physical oceanographic methodologies with those of behavioral ecology. Examination of organismal response

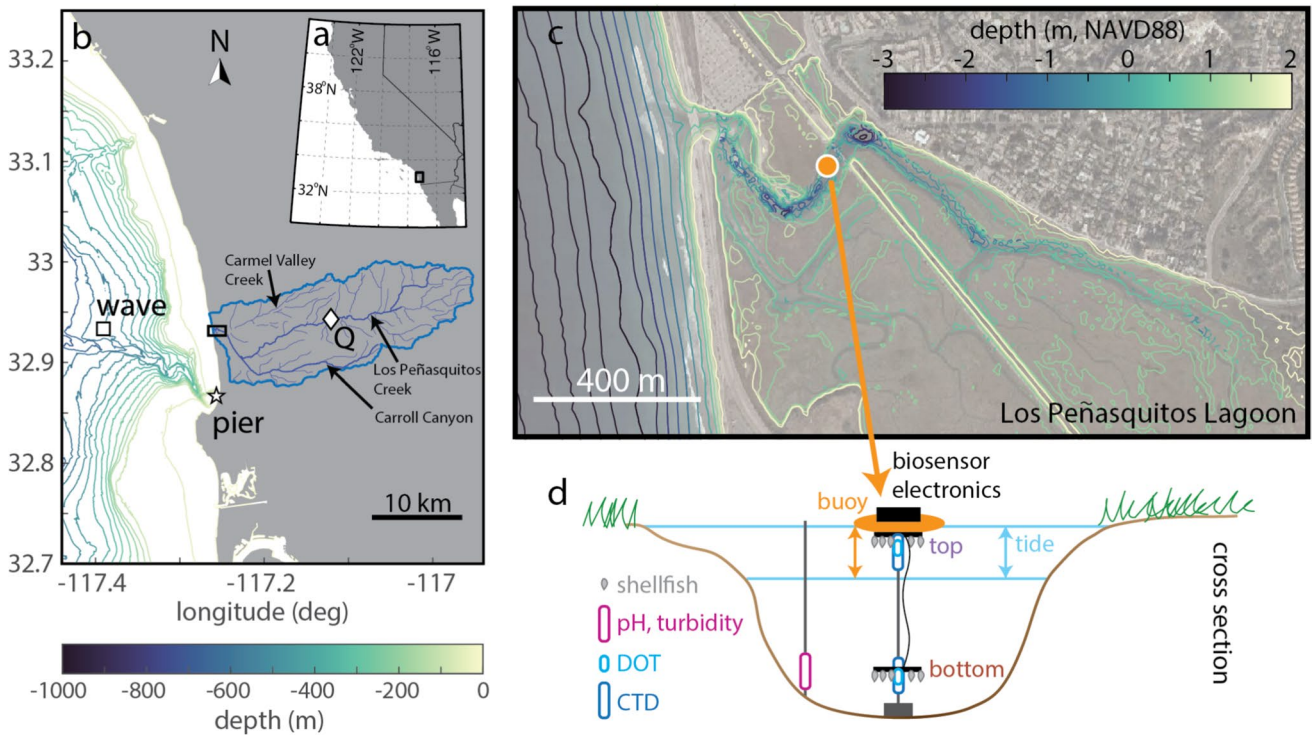

Fig. 1 Maps and schematics of Los Peñasquitos Lagoon (LPL) study site. **a** Inset map of California, with the study location on panel b indicated with a rectangle. **b** Closer view showing the watershed, contours of offshore bathymetry, and locations of the CDIP wave buoy [square], the Ellen Browning Scripps Memorial Pier (NOAA tide gauge, irradiance data [star]), the upstream USGS flow gauge [diamond], and the study site shown in c indicated with a rectangle. **c** Contour map of the LPL topography and nearshore bathymetry overlain on a Google map satellite image. The mooring location is indicated with an orange disc, at approximately $32.93337^\circ N$ and $-117.25716^\circ E$. **d** A schematic of the LPL channel cross section and the mooring. Note that the view is facing upstream, and the pH and turbidity sensors (at the NERR LPL NW station) are by the northwest stream bank offset across the estuary by less than 10m

across a very wide range of parameters is made possible by virtue of the estuary type and by having sensors located near-surface and near-bottom across a strongly stratified water column. This work addresses key knowledge gaps by utilizing long, high temporal resolution data, and extensive in-situ co-located environmental and water quality variables. Specifically, we hypothesized and found that:

1. Oysters near the surface have distinct valve gape behavior from oysters near the bottom of the water column, related to water column stratification.
2. Oyster valve gape varies periodically on diurnal, tidal, and fortnightly time scales, and so will have relationships with variables that are also periodic on those timescales due to known physical processes.
3. These relationships may be nonlinear, and correlated with each other, so a qualitative analysis of their joint distributions is necessary to understand to which variables the oysters are directly responding.
4. The majority of oyster valve gape variance can be explained by some time-varying combination of the concurrently measured variables.

Methods

Field Site

Los Peñasquitos Lagoon (LPL) is a small LIE and ICE in northern San Diego, southern California, USA. The LIE nature and strongly stratified, tidal dynamics of LPL inherently provide a wide range of environmental conditions. The inlet closes at least once seasonally, during which time the conditions respond strongly, including extended periods of hypoxia and overall estuarine freshening (Harvey et al., 2023). Precipitation, and resulting freshwater runoff, occurs mainly in late winter and early spring, during occasional storms. LPL is shallow, with a maximum depth of approximately 4 meters. The main channel is no wider than 70 meters, and the entire estuary covers about 2 km^2 Fig. 1(c). The inlet crosses a beach consisting of sand and cobbles. Inlet closures occur mainly during late spring due to accretion caused by large waves coincident with minimal river flow (Elwany, 2011; Harvey et al., 2023). Since 1932, the inlet has been constricted under a bridge as part of the construction of Highway 101 / North Torrey Pines Road, which

has led to more frequent closures. LPL is the outlet of a roughly 255 km^2 watershed which includes Carmel Creek, Carroll Creek, and Los Peñasquitos Creek Fig. 1(b).

Prior to development by western settlers, LPL was a predominantly open estuary. As a result of increased closures caused by the highway berm (originally built in 1915 and modified in 1932) and increased year-round urban runoff, the salt marsh and salt flats of LPL have largely been replaced by brackish wetlands (Beller et al., 2014). These changes have led to increased occurrence and breeding of mosquitos which are vectors for viruses that cause human encephalitis, e.g., the West Nile Virus. Moreover, inlet closures result in rapid hypoxia at depth and upstream flooding risk. The 2015-2016 El Niño led to more frequent and severe mouth closures, indicating that the estuary state is sensitive to climate conditions (Harvey et al., 2020). To maintain ocean-estuary water exchange, and prevent ecological collapse, sediment dredging is performed when the inlet is closed or is near closing. Dredging is done at least once a year, but has been done up to 6 times in one year (2016). The cost of a single dredging is $115,000 to $130,000 (Harvey et al., 2023; Mike Hastings, personal communication). Each dredging moves between 2,000 and 30,000 m^3 of sediment (Crooks et al., 2019). During the 2020 Southern California harmful algal bloom, following the conclusion of the sensor deployment investigated in this study, LPL suffered a mortality event of fishes and invertebrates, associated with intermittent hypoxia, and abnormally high pH followed by abnormally low pH (Skelton et al., 2024). Mouth management decisions are applied using real-time measurements of dissolved oxygen and water levels as well as other factors such as mosquito presence. Restoration projects in LPL focus on increasing tidal influence and salt marsh in the back of the lagoon (Los Peñasquitos Lagoon Enhancement Plan, 2018).

Instrumentation

The oyster mooring was deployed in the main estuary channel upstream of the mouth and the first two bends Fig. 1(c) on November 25, 2019 and recovered on April 9, 2020 (136 days). This deployment period was chosen to monitor the oysters through the winter time when freshwater input is present, and into the spring when there is potential for inlet closure due to sill build up following winter storm waves, all of which are conditions that were likely to cause changes in flow and water quality that might drive animal behavioral responses. Data collection stopped earlier than planned due to water intrusion in the data logger housing. The mooring was redeployed on May 18, 2020 during an inlet closure, however all instrumented oysters died within 5 days. This second deployment is not included in the main analysis of this study, and is used qualitatively in the discussion section.

The mooring was anchored using lead weights, and the top of the mooring line was attached to a foam boogie board. The total mooring line length was about 5 meters to allow for tidally varying water levels and scope during strong currents. Sensors were attached to the mooring line using hose clamps and zipties. Near-bottom sensors were attached about 0.5 meters above the bottom, suspended by a subsurface float. Near-surface sensors were attached about 0.2 meters below the surface. The water column depth at the mooring varies from around 1 to 2.9 meters with the top/bottom sensors varying from 0.3m apart to 2.2m apart.

On the mooring, both near-surface and near-bottom, was a Seabird SBE 37 CTD to measure salinity, temperature, and depth, and a Precision Measurement Engineering Mini-DOT to measure DO concentration. The CTDs sampled every five minutes. The DO sensors sampled every minute. Sensors were affixed to *Crassostrea gigas* oysters originating from the shallow banks of LPL. This species is non-native, having been introduced sometime after 2005, and was chosen due to its prevalence in this system (Crooks et al., 2015). Ten oysters were deployed, five near the water surface (just beneath a floating platform), and five near the estuary bottom Fig. 1(d). Two of the near-bottom oysters were not included in the analysis, because one oyster died soon after deployment, and the other oyster's sensor malfunctioned. Oyster shell valve opening and closing was monitored using a Hall effect sensor (A1395, Allegro Microsystems, Manchester NH) and neodymium magnet (6.35 mm diameter, 1.59 mm thick) glued to the opposing shell valves (Miller, 2022; Wilson et al., 2005), such that changing distance between the Hall effect sensor and magnet as the shell opened and closed was registered as a changing voltage. Voltage values were recorded by a custom data logging device based on Arduino open-source hardware designs (https://github.com/millerlp/MusselGapeTracker). Raw voltage values were recorded at 5 s intervals, and were converted to estimates of opening distance (units of mm) and then to relative opening (gape fraction, 0 for completely closed to 1 for completely open for each individual oyster) using the methods described in Miller and Dowd (2017). The original 5 second interval data were decimated to 1 minute intervals for subsequent analysis.

Just northwest of the mooring (less than 10 meters away) is a National Estuarine Research Reserve (NERR) monitoring station which includes pH and turbidity measurements, sampled every 15 minutes near the bed (Station LPL NW, data accessible at http://torreypines.trnerr.org/). Cross-shore and along-shore radiation stresses (S_{xx} and S_{xy} respectively) were sampled hourly from the Coastal Data Information Program (CDIP) monitoring and prediction point

offshore of Torrey Pines Beach (site D0587). River flow, sampled every 15 minutes, was obtained from a USGS gauge upstream on Los Peñasquitos Creek Fig. 1(b). Global horizontal irradiance was obtained from the National Solar Radiation Database's Physical Solar Model version 3, at the nearest spatial bin to the mooring. The model output has a 2 km spatial resolution and a 30 minute temporal resolution. Observed irradiance from the Ellen Browning Scripps Memorial Pier in La Jolla near the field site compared well to this model product, but was not available for the full time series, and so was not used as part of this study. Offshore water level (sampled hourly), wind direction and speed (sampled every 15 minutes), were obtained from the NOAA tide and meteorological station (station ID 9410230) located on the Ellen Browning Scripps Memorial Pier, about 7.5 kilometers south of the mooring Fig. 1(b).

Data Analysis

Data Preparation

To enable ease of analysis, all time series were cleaned, filtered, and subsampled to 30 minute intervals. Gaps in the oyster valve gape fraction time series, no longer than two hours, were interpolated using an autocorrelation kriging method. Data were 60-minute low pass filtered with a first order Savitzky-Golay filter (to avoid phase shifting and ringing typical of convolution based filters) and then subsampled to 30 minute intervals so that all time series were aligned with uniform time stamps, resulting in 6543 subsamples in each time series. Sub-sampling following filtering produces values that represent 60 minute means of the 1-minute sampled oyster valve gape fraction. The 30-minute processed time series was tidally averaged (using a low-pass Godin filter described in Godin et al. 1981) and the higher frequency residual was calculated by subtracting the tidally averaged data from the 30 minute processed data.

Spearman Correlations

To determine which environmental variables may be significant drivers of oyster valve gape behavior, a cross-correlation analysis was performed. Spearman correlation was chosen rather than Pearson correlation because the oyster valve gape data is not normally distributed. Variables with which many of the oysters have similar values of both the lag time of the central peak correlation, as well as their central peak correlation values, are determined to be significant environmental drivers of oyster valve gape behavior. Pairwise Spearman cross correlations between the oyster valve gape fraction time series and environmental data (water depth, insolation, northerly and easterly wind velocity components, pH, turbidity, cross-shore and along-shore wave radiation stresses, river flow, salinity, temperature, and DO) were calculated. Although they may not directly influence one another due to stratification, near-surface oyster valve gape was compared with the near-bottom measurements of pH and turbidity because prior work in LPL, as well as data shown here, indicate that surface and bottom parameters still co-vary due to the strongly tidal nature of the estuary (Harvey et al., 2023).

Different estuarine processes influence water properties on tidal and tidally averaged time scales, with the tidally averaged time scale relevant to the residence time of nutrients and pollutants (Geyer & MacCready, 2014). For this reason, the cross-correlation analysis was performed for the tidally averaged and high-frequency residual (i.e., tidal and higher) separately, as well as for the full 30 minute processed data (to determine the overall most correlated variables). The most consequential peak in the cross-correlation, chosen between the two prominent peaks around a lag of zero, was chosen as the central peak correlation and lag time. Statistical significance of the central peak correlation is defined as the likelihood that this lag would still be the central peak given another random sampling of the data. This significance was calculated using a Monte Carlo surrogate method (N=200). Surrogate data were generated using a random phase technique, to preserve the spectrum of the measured data.

Phase Distributions

In order to determine the relationships between tidal and diurnal solar cycles and oyster valve gape, and characterize the distinct behaviors of near-surface and near-bottom oysters over these cycles, tidal and diurnal phase distributions of oyster valve gape were calculated. Similarly to Harvey et al. (2023), tidal phase was defined between two offshore higher-high water levels. Tidal cycles that were not clearly semidiurnal (where a higher high tide was not followed by a lower high tide) were not included (13 tidal cycles). Incomplete tidal cycles at the beginning and end of the oyster deployment were also not included.

Diurnal phase was found from solar irradiance by aligning solar noon and solar midnight from the clearsky GHI provided by the PSM. Distributions of oyster valve gape behavior were determined in 100 phase bins, with respect to these definitions of the tidal, and diurnal phases. All surface oysters and bottom oysters were included in these distributions. This resulted in 122 tidal cycles, and 133 diurnal cycles. The effect of the fortnightly spring neap cycle was examined by splitting the tidal cycles into two even groups (61 cycles each) by tidal range, where the spring and neap groups had mean tidal ranges of 2.11 meters and 1.32 meters,

respectively before calculating the phase distribution. These phase distributions were analyzed in lieu of spectral analysis to observe nonlinear and harmonic effects, building on the linear analysis in Tran et al. (2011).

Joint Distributions

To examine the shared influence of two variables on oyster valve gape, three dimensional joint distributions were also generated for near surface and near bottom oysters. The median oyster valve gape in each 2-dimensional bin was calculated to show a typical value of oyster valve gape as a function of these variables. The joint distribution of oyster valve gape with DO and salinity was chosen due to their similar cross correlation coefficients and lag times, as well as their similar tidal phasing (Harvey et al., 2023), so the joint distribution can show their conditional relationships. The joint distribution of oyster valve gape with pH and turbidity was similarly chosen due to their similar cross correlation coefficients. In addition, both pH and turbidity were only measured near the bottom of the water column, so further examination of these joint distributions can clarify the significance of their relationships with near surface and near bottom oyster valve gape behavior.

Multivariate Models

In the absence of direct measurements, it would be useful to have a model to predict oyster valve gape as a function of more commonly monitored environmental conditions. Here we test a few nonlinear models and compare them to a linear model. We tested a set of models that most directly tests the hypothesis that oyster valve gape is dynamically dependent on the local state of the environment. Specifically we tested three variations of Empirical Dynamic Modeling (EDM), using k-nearest neighbor (knn) regressor from the scikit-learn Python library, and two models from the pyEDM Python library, namely Simplex and S-Maps (Sugihara, 1994; Sugihara & May, 1990). Note that all previously described analysis was done using MATLAB however this analysis was done using Python because there is no MATLAB equivalent to these EDM Python libraries. Six skill metrics are used to evaluate the linear and nonlinear models: the coefficient of determination (R^2), root mean square error (RMSE), Willmott skill (Willmott, 1981), model bias, Pearson's correlation, and Spearman's correlation.

The theoretical basis for EDM is mechanistic, and only has predictive power when the variables chosen belong to the same dynamical system, and are dynamically causal (Deyle & Sugihara, 2011; Sugihara et al., 2012). By choosing the right set of observable environmental variables and their time delays to define an embedding space, the attractor that corresponds to the full dynamics of the system will be reconstructed. This enables accurate prediction of future states by searching for nearest neighbors on this multidimensional attractor. Briefly, the Simplex model calculates the centroid of the nearest neighbors of the prediction point on the attractor as an estimate of the target point, and the S-Map model calculates a linear regression of the nearest neighbors with the target variable, which provides a slightly different estimate than the Simplex model. We also tested the knn regressor, which uses a different distance weighting for the nearest neighbors (the knn regressor uses an inverse distance weighting, while Simplex and S-Maps use an exponential weighting). These three variations of EDM were chosen because, although oyster valve gape behavior is assumed to be similar when environmental conditions are similar, the type of locality in the state space (distance weighting, local functional relationship) is unknown. Comparison among these variations is necessary to determine the most appropriate EDM model for this dataset. Since S-Maps calculates local linear regressions in the state space of the chosen variables, it also provides predictions of the relative contribution of each variable to predictions of oyster valve gape fraction.

The same embedding was used for all of these models. Filtered valve gape fraction for the surface oysters was predicted as a function of filtered simultaneous measurements of near surface DO and salinity, near-bottom pH, solar irradiance, and near-bottom turbidity, as well as the values of these variables 18 hours previously. This set of variables was chosen based on an assessment of the values of the valve gape-variable cross correlations found previously, as well as the assumption that oyster valve behavior is dynamic, and is therefore a function of previous system states. The lag value was chosen based on the peak lag of the autocorrelation of the mean valve gape fraction of the surface oysters. The number of nearest neighbors used for each prediction was twenty percent of the number of points in the training set. This value was chosen based on a brute force search for the value that gave the best model skill. Valve gape fraction and the predictor variables were filtered using a 6-hour causal half-hamming filter. The data were then subsampled to a 1.5-hour interval. This filtering and subsampling reduced noise and model runtime, respectively, while preserving features on timescales in the data that are known to influence valve gape behavior, such as the diurnal and tidal timescales (Tran et al., 2011). Subsampling additionally ensures that data points are maximally independent, which is particularly important for such a short time series where a rigorous test of the model requires evaluation of skill metrics on many randomized data shuffles.

If more data collection would lead to better nonlinear models, i.e. the state space is not yet optimally resolved,

then we expect that with increasing training library size, nonlinear model skill metrics would continue to improve, while linear model skill would increase more slowly or level off. In order to evaluate the benefit of increased data collection on model skill, the models were evaluated by shuffling the data 100 times, and fitting the models on training libraries of various sizes, from 5 to 85% of the total length of the dataset. Each instance was tested on an out-of-sample set of shuffled data (15% of the total length of the dataset), as well as an in-sample set of data (30% of the training library used for that model instance). Data shuffling prevented biases caused by the uneven temporal distribution of states (e.g. some segments in the time series have more open oyster valve gape states than closed states). In-sample testing was used to evaluate model overfitting (skill metrics for in-sample testing should be comparable to the skill metrics for out-of-sample testing).

Results

Distributions of Oyster Valve Gape and Environmental Time Series

Figure 2 shows the time series and distributions of 30 minute processed (a-b) and tidally averaged (c-d) oyster valve gape, with the 30 minute processed time series showing a two day segment of the record to highlight its variability. On the shorter timescale Fig. 2(a-b), variability between individual oysters is observed. However, within each set, oysters at the same depth in the water column behave similarly to one another and exhibit different patterns of opening and closing between the surface vs. the bottom group. The distributions show both depth groups experienced bimodal distributions with a peak at fully closed (0 gape fraction) and a broad peak centered around a gape fraction of 0.5 Fig. 2(b). The distributions also show that the surface oysters were open less frequently than the bottom oysters. On the tidally averaged timescale, each oyster behaved similarly to those within the same depth set Fig. 2(c-d), and the surface vs. bottom oyster sets followed each other fairly closely until late February, when the two oyster sets began to show an inverse relationship in their gape behavior. When the tidally averaged time series shows a high gape fraction it reflects a time period when oyster closures only occur briefly each day/semi-diurnal period (see for example the shorter time series in panel a), however when the tidally averaged time series has a valve gape fraction near zero, that indicates that oysters were closed over the majority of the semi-diurnal period. All oysters were predominantly closed at the start and end of December 2019 and predominantly open through January and most of February 2020. The surface oysters were closed for most of the time in March and April Fig. 2(c), which is reflected in the tidally averaged distributions Fig. 2(d).

The full time series of oyster gape and all environmental variables are further examined by plotting their fields by time of day versus day (see Figs. 3 and 4). In this view,

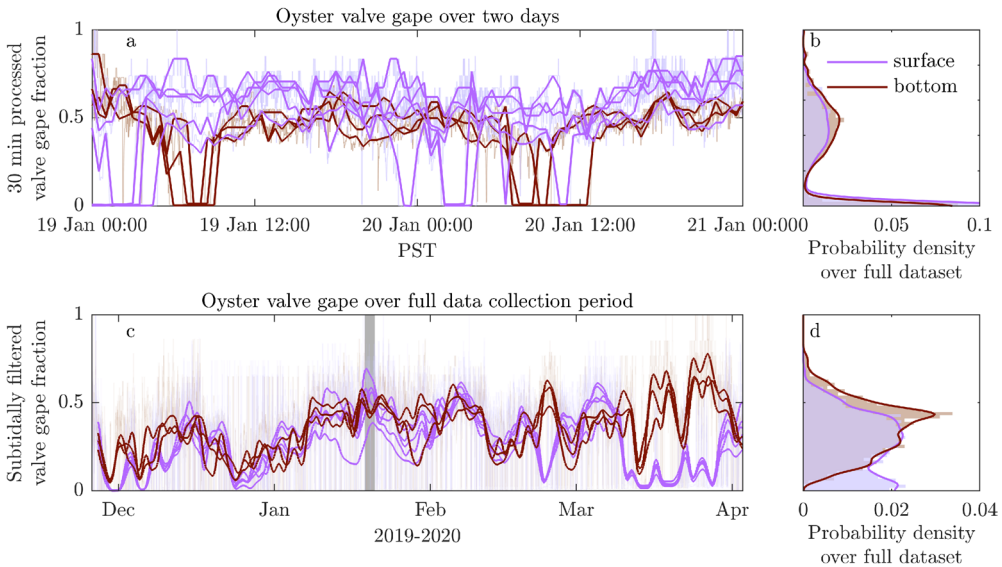

Fig. 2 Time series and distributions of *Crassostrea gigas* valve gape. The vertical axes on all panels shows the fractional valve gape, where zero indicates that an oyster is fully closed, and one indicates that an individual oyster is at its maximum gape that was observed over the entire data collection period. **a** 2-day snippet of 30 minute processed valve gape. The raw time series is shown faintly in the background. **b** The distribution of the full 30 minute processed time series. **c** Tidally averaged valve gape over the full 4.5 month record, with its corresponding distribution at the right. The vertical gray bar highlights the time period shown in panel **a**. 30 minute processed time series are shown faintly in the background of **c**. **d** The distribution of the full tidally averaged time series

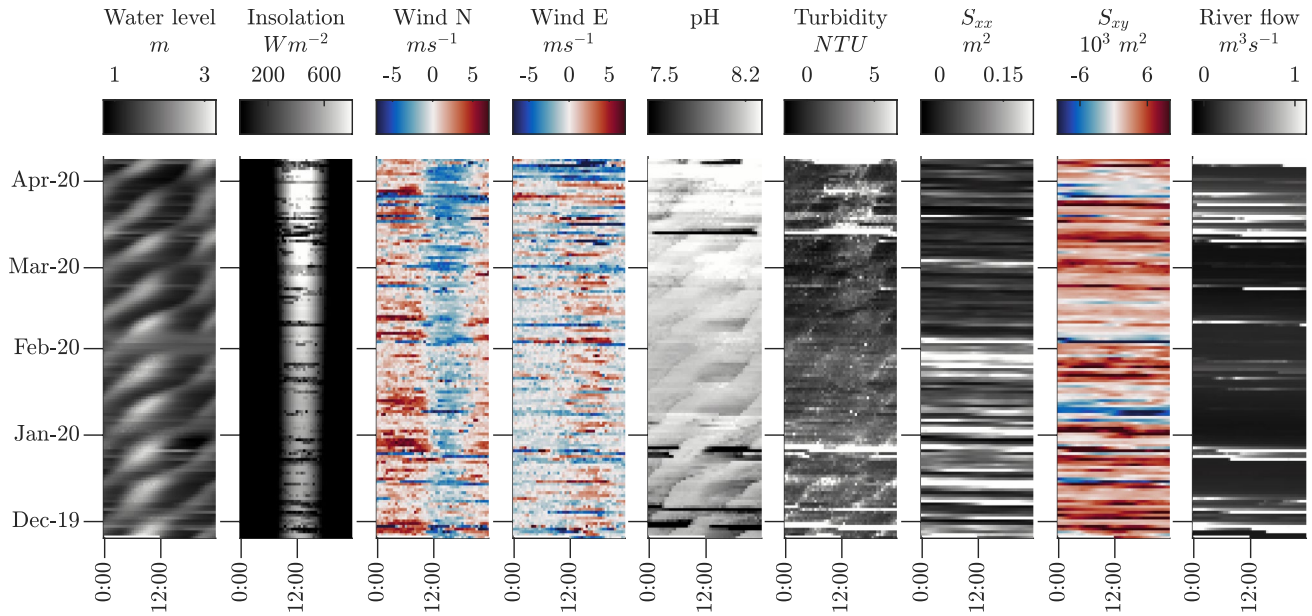

Fig. 3 Time series of 30 minute processed environmental variables measured in or near to Los Peñasquitos Lagoon from late November 2019 through April 2020. The variables shown from left to right are water level (m), Solar irradiance (Wm^{-2}), northerly and easterly wind speeds (ms^{-1}), pH, turbidity (NTU), cross-shore and alongshore radiation stresses S_{xx} and S_{xy} (m^2), and river flow (m^3s^{-1}). Time of day is shown on the horizontal axes, and calendar day is shown on the vertical axis. Displaying the data by both time of day and time highlights diurnal features as vertical stripes across the figures and tidal (semi-diurnal) features as diagonal lines. Event-scale features appear as horizontal stripes. Note that the color bars for turbidity and river flow are capped below their maximum values to highlight their variability

diurnal processes will show up as vertical stripes, tidal processes will show up as diagonal stripes, and event-scale variability will show up as horizontal stripes. This is most easily seen on the diurnally forced solar irradiance, which results in strong vertical stripes on Fig. 3b. Wind forcing is strongly diurnal. These figures also highlight well known high vertical stratification (Fig. 4 'Surface-Bottom Difference' in salinity) (Harvey et al., 2023), and a diurnal phase shift in surface vs. bottom heating (Fig. 4 'Surface-Bottom Difference' in temperature). Water level is tidally forced and thus shows diagonal stripes on Fig. 3a. Waves and river discharge are dominated by event-scale variability. It is also clear that events influence other water quality parameters as expected such as salinity and DO, which clearly vary with river discharge events. The other variables show a mixture of diurnal, tidal and event variability (pH, turbidity, DO, salinity, temperature).

The time series in Fig. 4 shows that oyster gape has diurnal, tidal, and event-scale variability. Overall, the bottom oysters are more open than the surface oysters (blue), particularly during these river discharge events Fig. 4. While a clear diurnal cycle is a bit hard to discern from each oyster set given overlap of semi-diurnal and event variability, the difference in the top and bottom oyster gape shows a clear diurnal pattern (i.e. surface oyster gape fraction being higher than bottom oysters during daytime hours and lower at night) suggesting a diurnal phase shift between each set. The surface oysters close during events when salinity and DO are low (horizontal dark lines across gape, salinity, and DO panels), coinciding with transient events of high river flow, low pH and high turbidity seen in Fig. 3 (horizontal lines at the same time periods).

Spearman Correlations

The strongest relationships of near-surface oyster valve gape are on the tidally averaged timescale, with salinity and dissolved oxygen at the surface Fig. 5. Salinity leads or lags behind surface oyster valve gape by no more than 2.5 hours. Dissolved oxygen leads surface oyster valve gape by no more than 14.5 hours. On the tidally averaged timescale, surface oyster valve gape is consistently positively correlated with insolation, pH, salinity, and dissolved oxygen, and is negatively correlated with water depth, turbidity, alongshore radiation stress S_{xy}, and river flow. On the tidally averaged timescale, near-bottom oyster valve gape has the clearest relationships with northerly wind speed (with lags ranging from 26.5 to 40.5 hours), positively correlated with easterly wind speed (with lags ranging from -2.5 to 13 hours), and negatively correlated with alongshore radiation stress (with lags ranging from -1.5 to 5 hours).

On the high-frequency (30 minute processed minus tidally averaged) timescale, the surface oysters have the strongest and most consistent relationships with insolation

(positive), temperature (positive), water depth (negative), and northerly wind speed (negative) (Fig. 6). Near-bottom oyster valve gape has the clearest relationships with insolation and temperature on the high-frequency timescale. Surface oyster valve gape leads temperature by about 5 hours, while bottom oyster valve gape leads temperature by an hour or less. Surface oyster valve gape is approximately in phase with insolation (lagging behind by an hour or less), while near-bottom oyster valve gape is negatively correlated with insolation, leading it by six hours.

The cross correlations of the 30 minute processed data reveal a more complex picture, with all variables but northerly wind and crossshore radiation stress S_{xx} having some statistically significant correlations with surface oyster valve gape (Fig. 7). Salinity, DO, river flow, pH, and turbidity have the overall strongest correlations with surface oyster valve gape. Bottom oysters overall have a weaker response to all variables, with some significant correlations with both wind components, alongshore radiation stress S_{xy}, and temperature.

Solar Phase Distributions

The surface and bottom oysters have distinct diurnal behavior Fig. 8. While the surface oysters are most open around noon, the bottom oysters are most open later in the day, near dusk. This is also seen on Fig. 4 bottom left panel. This phase offset can also be seen in Fig. 6 with the lagged correlations between each oyster and temperature. These correlations indicate that peaks in oyster valve gape preempt maximum temperature by about an hour for the bottom oysters and by about four hours for the top oysters. The peak daily temperature of coastal water occurs in the late afternoon/early evening, a few hours after the peak insolation at solar noon (Rasmussen et al., 2020), a time difference that mirrors the lags seen here. This distinct behavior between surface and bottom oysters is consistent at the quartiles of the distributions (Fig. 8).

Tidal Phase Distributions

The tidal phase distributions of oyster valve gape also shows distinct behavior between the surface and bottom oysters (Fig. 9). Both sets of oysters have a lower median valve gape around the higher-low tide ($\frac{3\pi}{2}$ in Fig. 9), although the surface oysters' response is far more dramatic. Both sets of oysters have a predominantly diurnal tidal pattern. Harvey et al. (2023) show the highest stratification of the tidal cycle around this higher-low tide in LPL, which is likely due to tidal straining during the ebb tides, and is commonly observed in estuaries (Geyer & MacCready, 2014; Stacey et al., 2001). Stratification results in less vertical mixing, possibly reducing food availability to oysters at both depths, through reduced mixing of phytoplankton to the lower water column and reduced mixing of nutrients into the upper water column. The surface oysters have a larger response to this since the stratification often leaves them in fresher water from upstream.

Median oyster valve gape fraction is greater during spring higher-high tides than during neap higher-high tides. Surface oysters close following spring lower-low tides and following neap lower-high tides (not shown). This may be a result of the estuary briefly losing high salinity inflow from the ocean due to a combination of the inlet sill and low water level at spring lower low tide, thus reducing the water and possibly nutrient flow around the oysters. Water level within LPL continues to ebb and freshen until around midway through the rising tide, indicating that the oysters are responding immediately to the changing tide (Harvey et al., 2023).

Joint Distributions

While correlation coefficients show which variables have relationships, the complex nature of those relationships is not easily quantified. Salinity, dissolved oxygen, and pH are positively correlated with surface oyster valve gape, while turbidity is negatively correlated with surface oyster valve gape. These relationships are all consistent with the oysters responding to tidal and episodic forcing, as these variables are all correlated with the tidal cycle in LPL (Harvey et al., 2023) and consistent with episodic storm forcing. To clarify the relative influence of these correlated variables on median valve gape fraction, we look at the joint distributions of median valve gape fraction with respect to dissolved oxygen and salinity, and pH and turbidity Fig. 10.

For oysters near the surface, when salinity is less than approximately 30 PSU, oyster valve gape has a dissolved oxygen threshold around 7 $mg\ L^{-1}$, above which oysters are most open. When salinity is higher, the oxygen threshold is lower, around 4.5 $mg\ L^{-1}$. This suggests that oysters respond to both oxygen and salinity, and that high values of either one is associated with open valve gape, even if the other is lower.

Oysters near the bottom of the water column similarly are more open when there is high salinity and high dissolved oxygen. The bottom oysters are more open when dissolved oxygen is greater than approximately 5 $mg\ L^{-1}$, and do not have a clear salinity threshold value. Although the bottom oysters spend more time within a narrower range of salinity (higher values) and dissolved oxygen than the surface oysters, the bottom oysters appear to be more willing to remain open in a broader range of salinity and dissolved oxygen concentration.

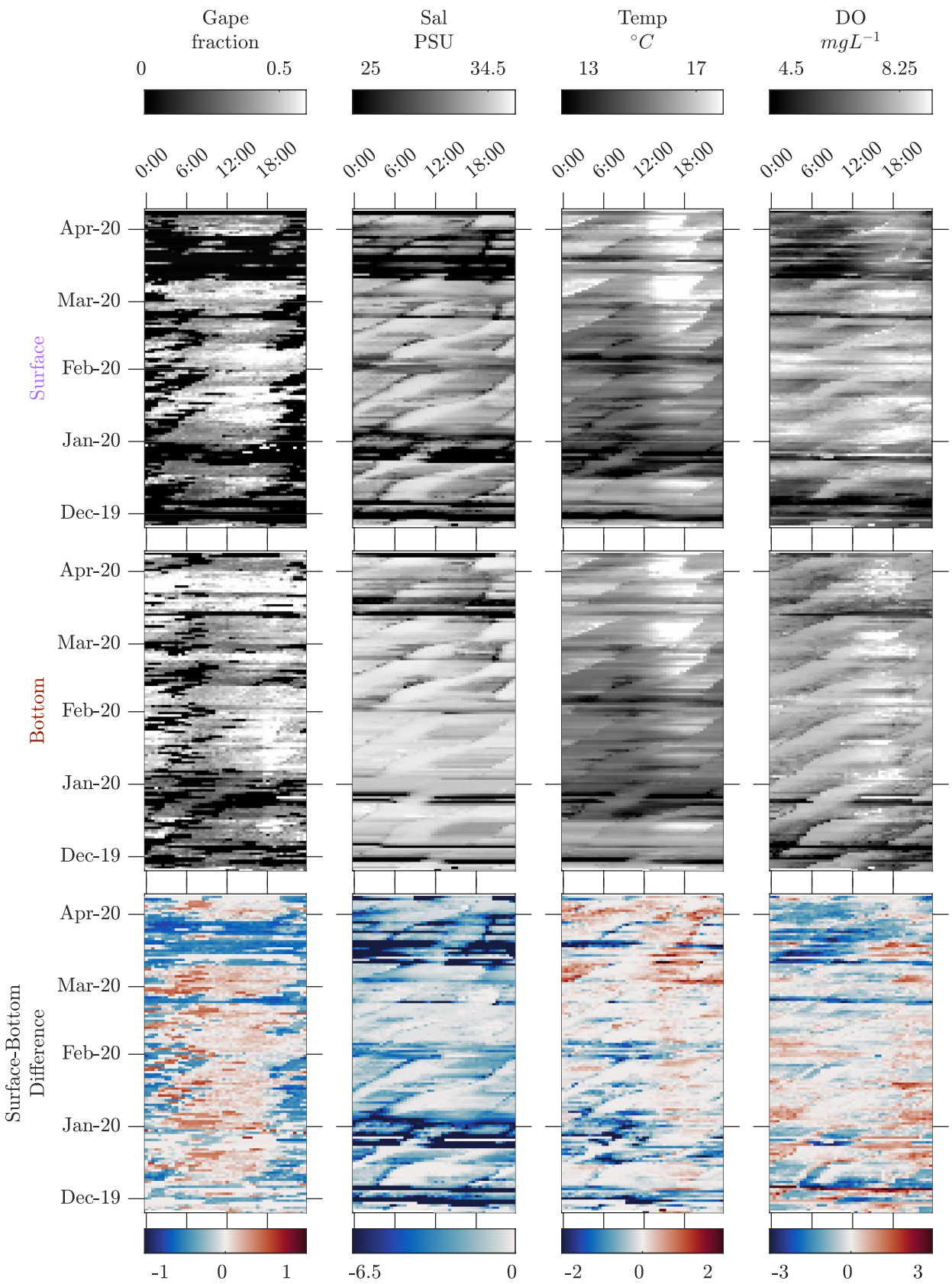
Gape
fraction
0
0.5
Sal
PSU
25
34.5
Temp
°C
13
17
DO
mgL⁻¹
4.5
8.25
0:00
6:00
12:00
18:00
Surface
Bottom
Surface-Bottom
Difference
Apr-20
Mar-20
Feb-20
Jan-20
Dec-19
-1
0
1
-6.5
0
-2
0
2
-3
0
3

Fig. 4 Time series of 30 minute processed data from the LPL mooring from late November 2019 through April 2020. The variables shown, each in its own column, are oyster valve gape fraction (labeled as Gape fraction), salinity (Sal, PSU), temperature (Temp, $^{\circ}C$), and dissolved oxygen (DO, mgL^{-1}). The top row labeled at the left in purple as 'Surface' shows the data from the surface sensors. The middle row, labeled at the left in brown as 'Bottom', shows the data from the bottom sensors. The bottom row, labeled at the left as 'Surface-Bottom Difference' shows the difference between the surface and the bottom sensors where positive (red) values indicate that the top sensors have higher values than the bottom and negative (blue) values indicate that the bottom sensors have higher values than the top. Time of day is shown on the horizontal axis, and day is shown on the vertical axis as done in Fig. 3. Compare to Figure 1 in Tran et al. (2011)

Surface oysters are most open when turbidity is below approximately 8 NTU, as long as pH is above approximately 7.8. Bottom oysters are more tolerant of higher turbidity than are the surface oysters when pH is high, with a threshold that increases linearly. Bottom oysters have a threshold pH of approximately 7.6, below which they are closed at all values of turbidity. It is important to note that here pH and turbidity are both measured near the bottom of the water column, so some differences in the upper water column may not be captured by this analysis with the surface oysters.

A joint distribution of median valve gape fraction with respect to pH and salinity (not shown) reveals that surface oyster valve gape is more dependent on salinity, while bottom oyster valve gape is more dependent on pH. The salinity cutoff for median surface oyster valve gape is approximately 27 PSU when pH is 8.6, increasing to approximately 33 PSU when pH is lower, at 7.4. The pH cutoff for median bottom oyster valve gape is approximately 7.9 when salinity is 18 PSU, decreasing to a pH of around 7.5 when salinity is 34 PSU.

Multivariate Models

Given the stronger relationships of near-surface oyster valve gape compared to that of near-bottom oyster valve gape, the multivariate models were only tested using data from the near-surface oysters. All models tested explained a large fraction of the variance (R^2), indicating that the chosen variables together explain surface oyster valve gape behavior (although not necessarily causally) Fig. 11. Using 80% of the full time series, or 108 days of data for the training library, the largest R^2 value across all models is 0.84, for S-Map. The smallest R^2 value is 0.41, for knn. Similar values for in and out of sample skill scores indicate that these models are not overfitting, and should generalize well to new data. S-Map provided the model with the highest skill, improving rapidly over the other models as the training set size increased, indicating the nonlinearity of the dataset, and that the state space is not yet fully resolved, and model performance will improve with new data in varying estuary conditions Fig. 11.

The time series of surface oyster valve gape fraction from March 1 to April 8 2020 is shown in Fig. 12 along with the predictions of one instance of each model, trained on data from December 26 2019 to February 28 2020 (a 70% / 30% training / prediction split). In this model instance, S-Map has the best skill scores ($R^2 = 0.48$, $RMSE = 0.14$, Willmott Score $= 0.84$, Bias $= 0.04$, Pearson's $\rho = 0.73$, Spearman's $\rho = 0.74$), followed by Simplex ($R^2 = 0.27$, $RMSE = 0.88$, Willmott Score $= 0.71$, Bias $= -0.33$, Pearson's $\rho = 0.61$, Spearman's $\rho = 0.67$).

The local regression coefficients produced through this S-Map model instance Fig. 12 reveal that out of all the predictor variables, dissolved oxygen has the largest contribution when the mean surface oyster valve gape is in a closed state (i.e., March 13-17, 18-21, and April 7-9). Throughout most of the rest of the time series salinity dominates in importance. Overall, simultaneous variables had larger coefficients than the lagged variables, except for lagged pH which briefly has larger coefficients than all variables except for salinity before and after the oyster closures. It is valuable to note that this time period shown includes widely ranging conditions with frequent freshwater input due to storms (see Figs. 3 and 4).

Discussion

This study focused on determining the relationship on tidally averaged and high-frequency time scales of oyster valve gape behavior in LPL with salinity, temperature, depth, and dissolved oxygen, as well as with nearby water quality and environmental conditions such as estuary pH and turbidity, solar irradiance, coastal water level, upstream flow rate, offshore wave radiation stress, and wind speed. The strongest relationships found were with tidally averaged salinity and dissolved oxygen (positive Spearman's correlation coefficients of approximately 0.6), specifically among the instrumented oysters near the surface of the water column. The oysters near the surface also responded to pH (positive correlation), turbidity (negative correlation), and upstream flow rate (negative correlation). These relationships are consistent with co-variance between the water quality variables expected during storms; freshwater input from storms (higher upstream flow rate) brings low salinity, lower pH, higher turbidity, and lower DO water into the estuary. Note that during these events is also when the water column is most stratified (see Fig. 4 bottom panel).

Bottom oysters appear far less sensitive to the measured environmental variables on either the tidally averaged or

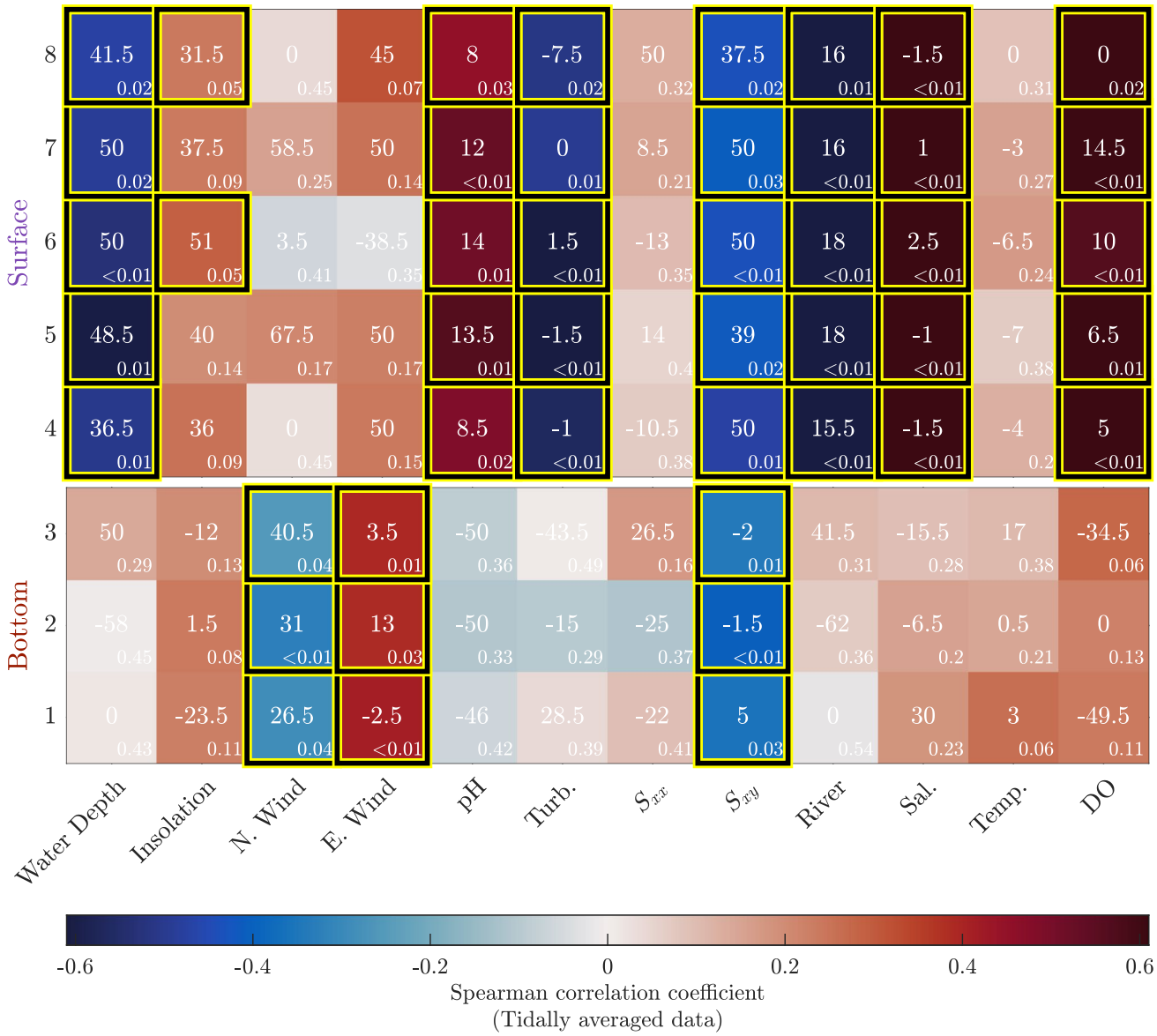

Fig. 5 Cross correlations between each oyster valve gape time series and each environmental variable at the tidally averaged time scale in LPL. The vertical axis shows each oyster (indexed 1-3 on the bottom of the mooring, 4-8 near the surface). Blue indicates a negative correlation, and red indicates a positive correlation. The large numbers in each cell are the lag in hours of the central peak. Positive lag values indicate valve gape lagging behind the environmental variable. The small numbers in the bottom right corner of each cell are the bootstrapped p-values. Cross correlations with p-values less than or equal to 0.05 are identified with bold black and yellow borders

higher frequency time scales. They do have statistically significant, although inconsistent, relationships with wind speeds and along shore radiation stress S_{xy}, particularly on the tidally averaged timescale, possibly due to the influence of these variables on bottom mixing and sediment transport and suspension. This is not reflected in the near-bottom oyster valve gape correlation with turbidity, which had no statistical significance. Despite this, near-surface oyster valve gape was found to have a significant correlation with turbidity. Estuaries tend to be more turbid at depth due to the effects of stratification and fluvial and tidal sediment transport (Uncles et al., 2002). The lack of a significant correlation between near-bottom oyster valve gape and turbidity can possibly be explained by acclimation of the near-bottom oysters to more turbid conditions, which has shown to be related to changes in the gills and pallial organs of *C. gigas* (Barillé et al., 2000; Dutertre et al., 2009). There also may be some relationships with other variables compounding this such as the fact that turbidity is highly correlated with river discharge which is shown to impact surface oysters more strongly than bottom oysters due to stratification. Correlations with wind speeds and alongshore radiation

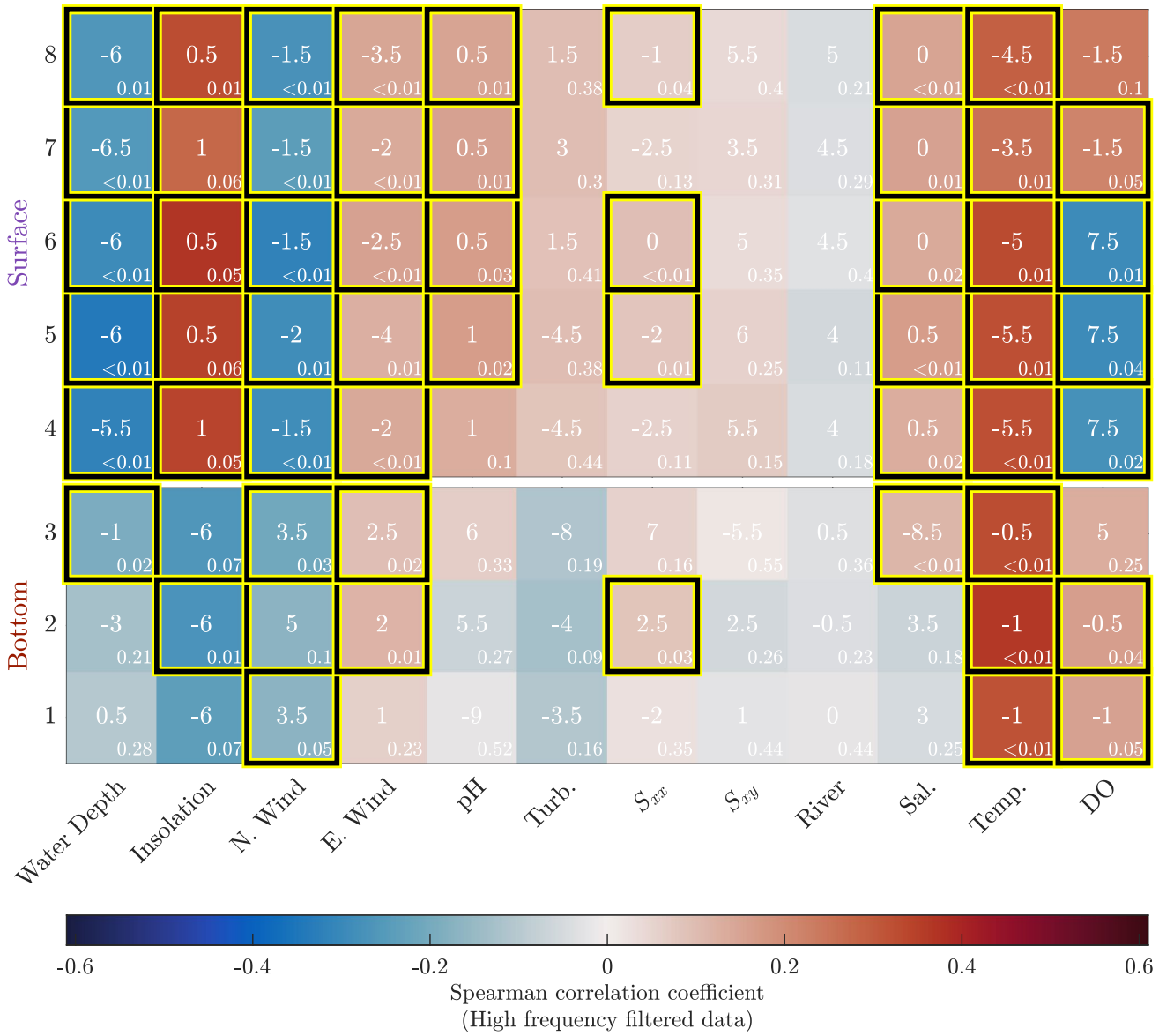

Fig. 6 Cross correlations of the high-frequency residuals (30 minute processed minus tidally averaged) of the tidally averaged time series of oyster valve gape and each environmental variable in LPL. The vertical axis shows each oyster (indexed 1-3 on the bottom of the mooring, 4-8 near the surface). Blue indicates a negative correlation, and red indicates a positive correlation. The large numbers in each cell are the lag in hours of the central peak. Positive lag values indicate valve gape lagging behind the environmental variable. The small numbers in the bottom right corner of each cell are the bootstrapped p-values. Cross correlations with p-values less than or equal to 0.05 are identified with bold black and yellow borders

stress for both the near-surface and near-bottom oysters are more likely indirect, all being influenced by episodic storm conditions.

The relationships shown through cross-correlations of oyster valve gape with temperature and insolation may be due to surface oysters responding to light exposure and solar radiation, rather than changes in temperature in the surrounding water. A cross correlation between surface and bottom temperature with insolation (not shown in this paper), gives a positive maximum correlation with solar irradiance at a lag of 4.5 hours. The surface oysters thus may be responding to light, or an associated variable such as phytoplankton abundance, while the bottom oysters are responding to temperature. However, solar irradiance was not measured at the bottom of the water column in this experiment, so directly determining the difference in light exposure between the surface and bottom oysters was not possible. These relationships are supported by the solar phase distribution, that show similar lags between the diurnal cycle of oyster valve gape and solar phase.

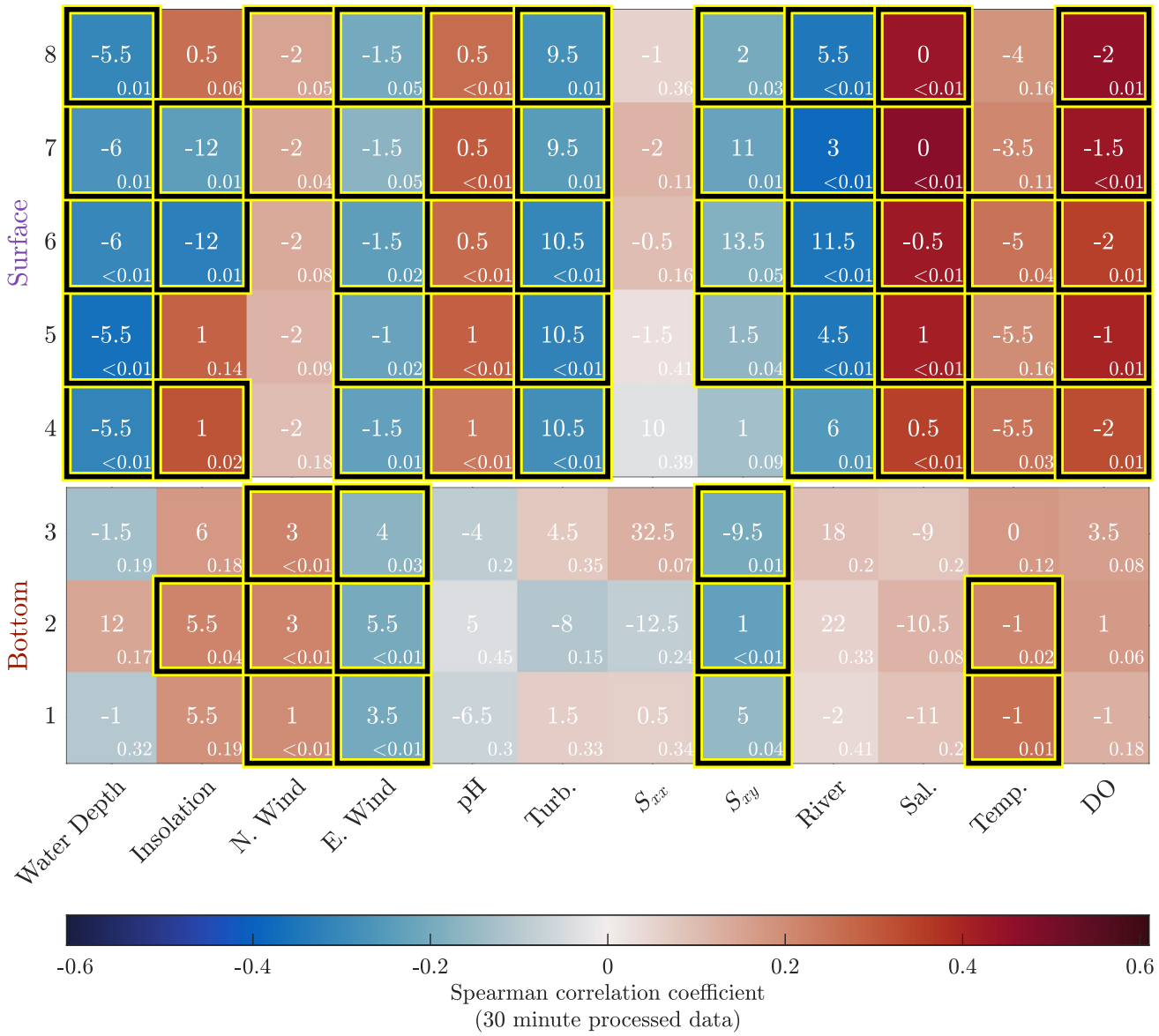

Fig. 7 Cross correlations of the 30 minute processed time series of oyster valve gape and each environmental variable in LPL. The vertical axis shows each oyster (indexed 1-3 on the bottom of the mooring, 4-8 near the surface). Blue indicates a negative correlation, and red indicates a positive correlation. The large numbers in each cell are the lag in hours of the central peak. Positive lag values indicate valve gape lagging behind the environmental variable. The small numbers in the bottom right corner of each cell are the bootstrapped p-values. Cross correlations with p-values less than or equal to 0.05 are identified with bold black and yellow borders

Phase distributions showed diurnal and tidal cycles in oyster valve gape behavior, consistent with research at other sites which have shown oyster valve gape to respond to both light and temperature (Casas et al., 2018; Tran et al., 2011). The diurnal cycle of near-surface and near-bottom oyster valve gapes are offset by approximately a quarter of a day, with surface oysters most open at midday, and bottom oysters most open in the evening. This may be attributed directly to temperature, or to other diel cycling of variables which were not measured during this field campaign, such as the vertical migration of plankton (on which oysters feed), which has been observed in other shallow estuaries, e.g. Hall et al. (2015). Valve gape behavior aligning with the tidal cycle appears consistent with oysters responding to tidal cycle variability in water quality parameters as observed in LPL, which is consistent with other tidally influenced, stratified estuaries (Harvey et al., 2023). Similarly, the stronger response of near-surface oysters relative to near-bottom oysters to their environmental conditions is consistent with stratification leading to overall more variable water quality conditions near the surface. The phase relationship of oyster valve gape with the tidal cycle suggests

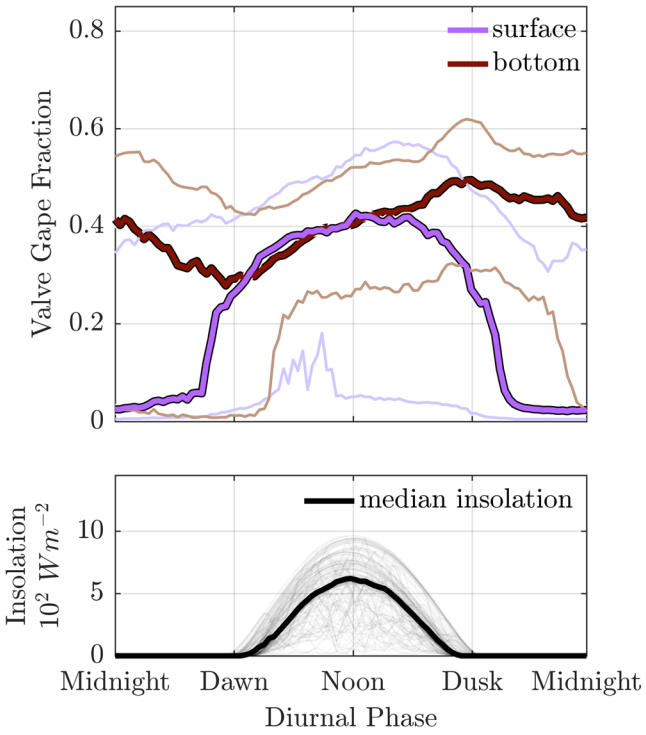

Fig. 8 Top panel: solar phase distributions of oyster valve gape fraction in LPL. The median surface and bottom oyster data are shown in purple and brown, respectively. Quartiles are shown in thin lines in their corresponding colors. Bottom panel: median diurnal insolation cycle, with lighter gray lines showing each instance of this cycle (N=133), including cloud cover

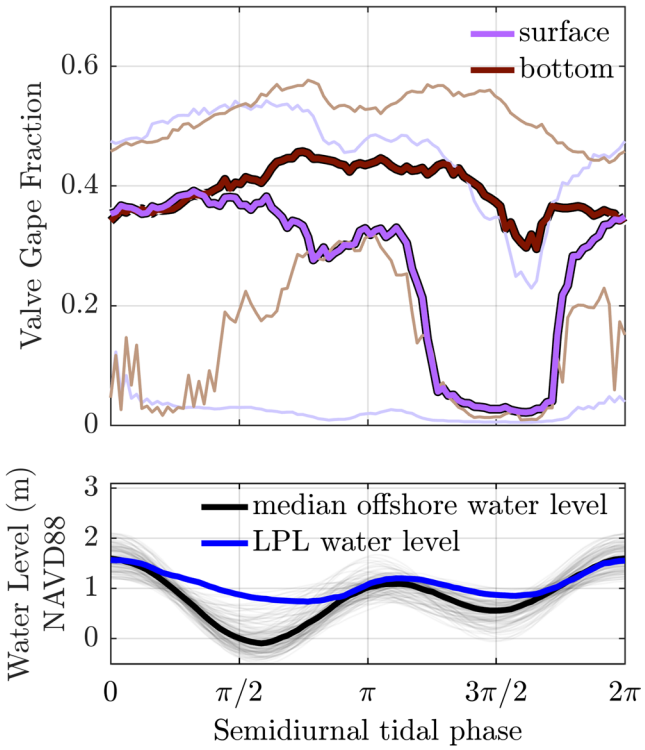

Fig. 9 Top panel: tidal phase averaged oyster valve gape in LPL. The median surface and bottom oyster data are shown in purple and brown, respectively. Quartiles are shown in thin lines in their corresponding colors. Bottom panel: The black line shows the median tidal cycle of the offshore water level, with lighter gray lines showing each instance of this cycle (N=122). The blue line shows the median tidal cycle of the water level measured at the mooring within LPL

that it is unlikely that oyster valve gape behavior has a direct dependence on water velocity. The observations in Harvey et al. (2023) show that velocity in LPL acts like a standing wave, 90° out of phase with water level. This, together with the predominantly diurnal tidal pattern of valve gape, indicates that oysters are responding to varying water properties, rather than to velocity.

This investigation of these observations shows a strong and consistent near-surface oyster response to multiple environmental parameters. The strongest response is with salinity and DO (with oysters preferring higher salinity and higher DO conditions with some thresholding effects). However, some of the conclusions drawn from this set of analyses are challenged by co-variance of the water quality parameters (for example, the lower salinity water has lower pH) and nonlinear relationships between oyster valve gape and the environmental variables.

The S-Map model was the strongest multivariate model tested, and should be explored further as a predictive monitoring tool. The local linear regression coefficients for each predictor variable provided through the S-Map model confirm the relative importance of simultaneous DO and salinity on oyster behavior. However, future models should take into account the non-negativity of oyster valve gape to produce more accurate predictions. It is worth noting that higher skill may be possible with an optimized lag for each variable, rather than a single lag applied to all variables. Including the lagged variables, compared with only including simultaneous variables), moderately improved skill scores for all models. The S-Map model improving the most, with an increase in the R^2 value by about 0.05. The overall greater performance of S-Map (and to a lesser extent Simplex) compared with the other models is a good indicator of the state dependence of system dynamics in LPL. Linear analyses assume separability of the effects of each variable, while models like S-Map and Simplex do not rely on this assumption. Accordingly, future analyses should explore a variety of nonlinear models.

Our study had some limitations that are important to consider when trying to contextualize this work for operational BEWS. To that end, we recommend the following improvements to our methodology. Given the significant inter-oyster variability in this study (including the death of one oyster at the beginning of the deployment),

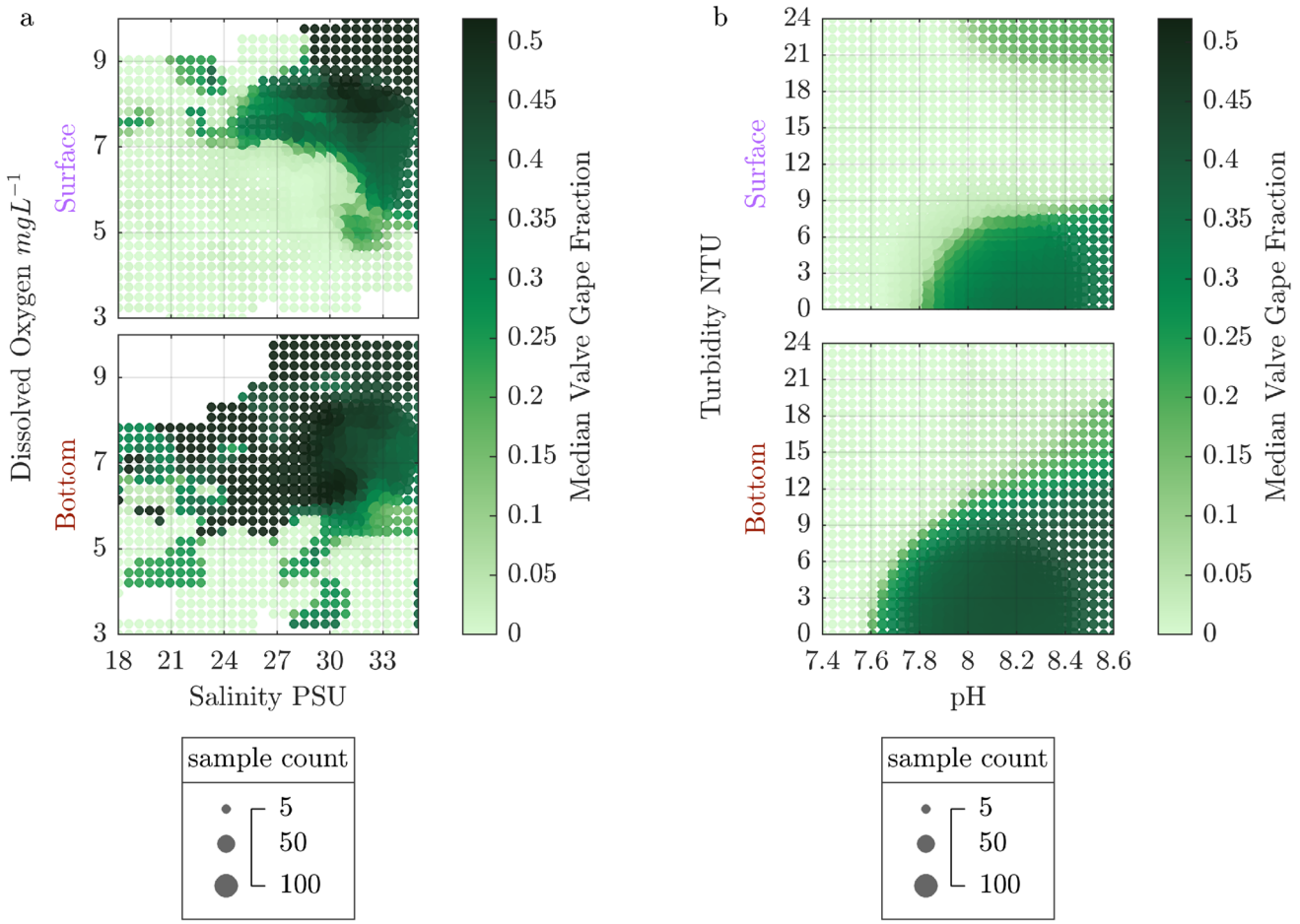

Fig. 10 **a** Joint distributions of median oyster valve gape as a function of salinity and oxygen in LPL. The top plot shows values for the oysters near the surface with near-surface measurements of salinity and oxygen, and the bottom plot shows the corresponding bottom measurements. **b** Joint distributions of median oyster valve gape as a function of pH and turbidity. The top plot shows values for the oysters near the surface with near bottom measurements of pH and turbidity (as these variables were only measured near-bottom), and the bottom plot shows the corresponding bottom oyster measurements. Larger dots indicate more measurements in that bin, varying continuously in size. Darker dots indicate a greater median valve gape fraction (i.e., oysters are more open)

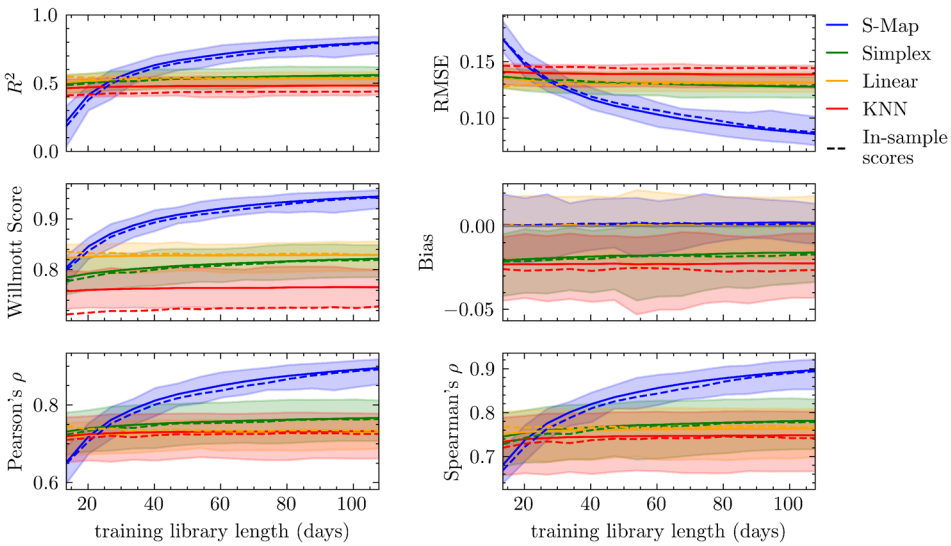

Fig. 11 Model learning curves, showing six different skill metrics for each of the four models as a function of the training dataset length. The x axis covers 5-85% of the full data set. Solid lines are the skill values when the model is tested on an out-of-sample set of data, while dashed lines indicate skill values when the model is tested on an in-sample set of data

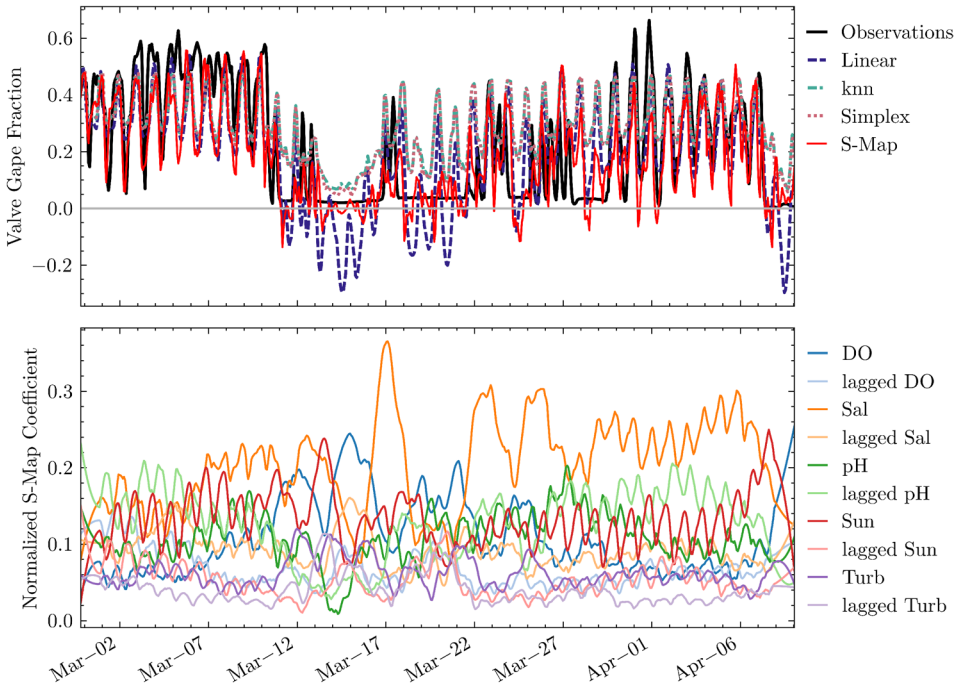

Fig. 12 Top panel: model predictions for February 29 2020 through April 9 2020 of 6-hour half-Hamming filtered mean surface oyster valve gape fraction, trained on 70% of time series (December 26 2019 - February 28 2020). Bottom panel: Normalized S-Map time varying coefficients for each variable used as predictors in the model, showing the relative contribution of changes in each variable to a change in oyster valve gape. For ease of visual interpretation, coefficients have been smoothed with a 3-day Hamming filter

oyster sample size should be increased as much as possible. We also suggest co-location of chlorophyll sensors (to assess phytoplankton, i.e., food source, abundance), and pH and turbidity sensors (here we were limited to pH and turbidity only near the bed).

To observe the oyster sensitivity to cross-channel and along-channel location, moorings could be deployed at multiple sites within a single estuary. Comparisons could also be made to native bivalve species to examine the extent to which their responses to environmental conditions differ in a changing estuary and climate (Skelton et al., 2024). Valve gape behavior of native species may also provide more effective indicators of pollution (Kelleghan et al., 2023). Finally, comparison across different sites would help elucidate if bivalve response varies by site or if there are some environmental cues that species respond to similarly across sites.

The deployment length should be increased as long as possible, or deployments should be overlapping, to observe and account for seasonal cycles in environmental parameters and oyster valve gape, such as that observed in Tran et al. (2011). Longer deployments will also allow observations before and during estuary inlet closures. Following the mooring deployment analyzed in this study, the mooring was redeployed with 8 new oysters during an inlet closure. The oyster mooring was not deployed while the inlet was closing. During the closure, compared to conditions when the inlet was open, near-surface and near-bottom salinity were low, near-surface and near-bottom temperature were high, and near-bottom dissolved oxygen and pH were low. All but two oysters (near-surface) on the mooring died within 5 days, before the inlet reopened. The redeployment occurred during a red tide (Skelton et al., 2024), creating particularly challenging conditions for the oysters. Continuous oyster valve gape observations spanning before, during, and after an inlet closure (or other high stress or mortality event) would be useful to determine oyster resilience to rapidly changing conditions, and provide timescales for biological response to inlet closures, stressors, and even for mortality. This information would be crucial to estuary management's decisions regarding response time to inlet closures before damage to the bivalve community.

All of these experimental modifications would help contextualize the usefulness of BEWS and the importance of local calibration of such systems. Beyond the use of BEWS to the environmental issue of inlet closures, there is the potential for their application in a variety of other management contexts (Andrewartha et al., 2015; Arroyo et al., 2022; Meira et al., 2024; Vereycken & Aldridge, 2023). This includes exploring the use of biosentinels in issues of local management importance, such as aquaculture (Wallace, 2023), invasive species assessment (Crooks et al., 2015), pollution monitoring (Mladenov et al., 2024), living shoreline creation (Ridlon et al., 2021), and developing indicators for tracking restoration success (Walker et al., 2025).

Conclusions

This study adds to the existing body of literature on how bivalves and benthic organisms respond to environmental changes in Los Peñasquitos Lagoon (Levin et al., 2023; Novoa et al., 2016) as well as to the body of literature on BEWS (e.g., Bae and Park 2014). The temporal and spatial scales measured and analyzed here provides new insight into bivalve behavior in this estuary, as well as more broadly as they can be used in BEWS. Our results show oysters responding to both salinity and DO with a strong impact of vertical stratification leading to differing responses of near-surface and near-bottom oysters. There is also a response to pH, turbidity, and a clear influence of both diurnal and tidal cycles (which due to the estuarine dynamics drive tidal variability in all water quality parameters). However, due to nonlinear responses and co-variance of environmental parameters, we tested several multivariate models. Multivariate nonlinear models such as S-Map show some promise in predictability and even data attribution, thus additional data collection to further test these models would be valuable. Combining further studies of this type with multivariate nonlinear models could allow managers to optimize which parameters are most critical to observe for establishing useful BEWS and provide insight into the use of similar BEWS across different systems.

Acknowledgements This work would not be possible without support and supplemental data from the Los Peñasquitos Lagoon Foundation, CA State Parks, the Tijuana River NERR, CDIP, SCCOOS, USGS, NOAA, the NERR SWMP, and the SIO Coastal Processes Group. In particular, we thank G Kalbach, M Hastings, J McCullough, M Cordrey, C Stafford, L Rose, D Smith, B Collins, R Flick, B Woodward, S Finnerty, and C Black. We also thank the two anonymous reviewers for their suggestions which have improved the manuscript.

Author Contributions NA performed the analysis, and wrote the original manuscript. SNG led project administration and supervision. SNG, LPM, and GS developed and supervised methodologies and analysis approaches. SNG, LPM, LAL, KAG, and JC conceived of the idea and obtained funding for the project. SNG, LPM, CN, LRM, and DW participated in field work. All co-authors participated in reviewing and editing the manuscript.

Funding This work has been supported by the National Estuarine Research Reserve (NERR) System Science Collaborative, which supports collaborative research that addresses coastal management problems important to the reserves. The Science Collaborative is funded by the National Oceanic and Atmospheric Administration and managed by the University of Michigan Water Center (NA19NOS4190058, subaward SUBK00016699). Biosensor and hydrodynamic sensor deployment was also supported in part by NOAA's National Centers for Coastal Ocean Science (NCCOS) Competitive Research Program under award NA18NOS4780172 to the Scripps Institution of Oceanography, University of California, San Diego, and by award NA16NOS4780205 to the CA Coastal Conservancy. NERR real-time data collection is supported by the NOAA Office for Coastal Management, award #NA24NOSX420C0043. This work is partially supported by grants from California (CA) Department of Parks and Recreation's Natural Resources Division and Division of Boating and Waterways, USC Sea Grant, CA Sea Grant, and NSF. This is CHRP contribution #270. This is contribution number 94 of the Coastal and Marine Institute Laboratory, San Diego State University. The statements, findings, conclusions, and recommendations are those of the participants/authors and do not reflect the views of NSF, NOAA, the Department of Commerce, or the Department of the Interior.

Availability of Data and Materials The datasets during and/or analyzed during the current study available from the corresponding author on reasonable request.

Declarations

Ethics Approval and Consent to Participate All research was conducted in accordance with institutional guidelines for animal care and use at the University of California San Diego and San Diego State University.

Consent for Publication Not applicable.

Competing Interests The authors declare no competing interests.

References

Andrewartha, SJ., Elliot, NG., McCulloch, JW., & Frappell, PB. (2015). Aquaculture Sentinels: Smart-farming with Biosensor Equipped Stock. *Journal of Aquaculture Research & Development*, *07*(01). https://doi.org/10.4172/2155-9546.1000393

Arroyo, C.L., Dionela, M., Ann Bautista, M.G., Concepcion, R., Vicerra, R.R., & Duarte, B. (2022). Biomonitoring technologies used in aquatic ecosystems: a systematic and trend analysis. In *IEEE 14th International Conference on Humanoid, Nanotechnology, Information Technology, Communication and Control, Environment, and Management (HNICEM)*, (pp. 1–5).

Bae, M.-J., & Park, Y.-S. (2014). Biological early warning system based on the responses of aquatic organisms to disturbances: A review. *Science of The Total Environment, 466–467*, 635–649. https://doi.org/10.1016/j.scitotenv.2013.07.075

Barillé, L., Haure, J., Cognie, B., & Leroy, A. (2000). Variations in pallial organs and eulatero-frontal cirri in response to high particulate matter concentrations in the oyster Crassostrea gigas. *Canadian Journal of Fisheries and Aquatic Sciences, 57*(4), 837–843. https://doi.org/10.1139/f00-012

Behrens, D. K., Bombardelli, F. A., Largier, J. L., & Twohy, E. (2013). Episodic closure of the tidal inlet at the mouth of the Russian River – A small bar-built estuary in California. *Geomorphology, 189*, 66–80. https://doi.org/10.1016/j.geomorph.2013.01.017

Beller, E., Baumgarten, S., Grossinger, R., Longcore, T., Stein, E., Dark, S., & Dusterhoff, S. (2014). *Northern San Diego County Lagoons Historical Ecology Investigation: Regional Patterns, Local Diversity, and Landscape Trajectories* (Tech. Rep. No. 722). San Fransisco Estuary Institute.

Borcherding, J. (2006). Ten Years of Practical Experience with the Dreissena-Monitor, a Biological Early Warning System for Continuous Water Quality Monitoring. *Hydrobiologia, 556*(1), 417–426. https://doi.org/10.1007/s10750-005-1203-4

Bub, S., Petschick, L. L., Stehle, S., Wolfram, J., & Schulz, R. (2025). Limitations of chemical monitoring hinder aquatic risk evaluations on the macroscale. *Science, 388*(6753), 1301–1305. https://doi.org/10.1126/science.adn5356

Casas, S. M., Filgueira, R., Lavaud, R., Comeau, L. A., La Peyre, M. K., & La Peyre, J. F. (2018). Combined effects of temperature and salinity on the physiology of two geographically-distant eastern oyster populations. *Journal of Experimental Marine Biology and Ecology, 506*, 82–90. https://doi.org/10.1016/j.jembe.2018.06.001

Costanza, R., d'Arge, R., de Groot, R., Farber, S., Grasso, M., van den Hannon, B., & Belt, M. (1997). The value of the world's ecosystem services and natural capital. *Nature, 387*(6630), 253–260. https://doi.org/10.1038/387253a0

Costanza, R., de Groot, R., Sutton, P., van der Ploeg, S., Anderson, S. J., Kubiszewski, I., & Turner, R. K. (2014). Changes in the global value of ecosystem services. *Global Environmental Change, 26*, 152–158. https://doi.org/10.1016/j.gloenvcha.2014.04.002

Cousins, M., Stacey, M. T., & Drake, J. L. (2010). Effects of seasonal stratification on turbulent mixing in a hypereutrophic coastal lagoon. *Limnology and Oceanography, 55*(1), 172–186. https://doi.org/10.4319/lo.2010.55.1.0172

Crooks, J., Crooks, K.R., & Crooks, A.J. (2015). Observations of the non-native Pacific oyster (*Crassostrea gigas*) in San Diego County, California. *California Fish and Game*, *101*(2).

Crooks, J., McCullough, J., Almeida, M., & Uyeda, K. (2019). *The Physical, Chemical and Biological Monitoring of Los Penasquitos Lagoon* (Tech. Rep.). Southwest Wetlands Interpretative Association and the Tijuana River National Estuarine Research Reserve.

de Groot, R., Brander, L., van der Ploeg, S., Costanza, R., Bernard, F., van Braat, L., & Beukering, P. (2012). Global estimates of the value of ecosystems and their services in monetary units. *Ecosystem Services, 1*(1), 50–61. https://doi.org/10.1016/j.ecoser.2012.07.005

de Zwart, D., Kramer, K. J. M., & Jenner, H. A. (1995). Practical experiences with the biological early warning system "mossel-monitor.". *Environmental Toxicology and Water Quality, 10*(4), 237–247. https://doi.org/10.1002/tox.2530100403

Deyle, E. R., & Sugihara, G. (2011). Generalized Theorems for Nonlinear State Space Reconstruction. *PLOS ONE, 6*(3), Article e18295. https://doi.org/10.1371/journal.pone.0018295

Dutertre, M., Barillé, L., Beninger, P. G., Rosa, P., & Gruet, Y. (2009). Variations in the pallial organ sizes of the invasive oyster, Crassostrea gigas, along an extreme turbidity gradient. *Estuarine, Coastal and Shelf Science, 85*(3), 431–436. https://doi.org/10.1016/j.ecss.2009.09.007

Elwany, M. H. S. (2011). Characteristics, Restoration, and Enhancement of Southern California Lagoons. *Journal of Coastal Research, 2011*(10059), 246–255. https://doi.org/10.2112/SI59-026.1

Fournier, E., Tran, D., Denison, F., Massabuau, J.-C., & Garnier-Laplace, J. (2004). Valve closure response to uranium exposure for a freshwater bivalve (Corbicula fluminea): Quantification of the influence of pH. *Environmental Toxicology and Chemistry, 23*(5), 1108–1114. https://doi.org/10.1897/02-604

Fuentes, C. M., Whitcraft, C. R., & Zacherl, D. C. (2020). Adaptive Restoration Reveals Potential Effect of Tidal Elevation on Oyster Restoration Outcomes. *Wetlands, 40*(1), 93–99. https://doi.org/10.1007/s13157-019-01166-7

Gale, E., Pattiaratchi, C., & Ranasinghe, R. (2007). Processes driving circulation, exchange and flushing within intermittently closing and opening lakes and lagoons. *Marine and Freshwater Research, 58*(8), 709–719. https://doi.org/10.1071/MF06121

Geyer, W. R., & MacCready, P. (2014). The Estuarine Circulation. *Annual Review of Fluid Mechanics, 46*(1), 175–197. https://doi.org/10.1146/annurev-fluid-010313-141302

Godin, G., Candela, J., & de la Paz-Vela, R. (1981). On the feasibility of detecting net transports in and out of Georgia strait with an array of current meters. *Atmosphere-Ocean, 19*(2), 148–157. https://doi.org/10.1080/07055900.1981.9649106

Hall, N. S., Whipple, A. C., & Paerl, H. W. (2015). Vertical spatiotemporal patterns of phytoplankton due to migration behaviors in two shallow, microtidal estuaries: Influence on phytoplankton function and structure. *Estuarine, Coastal and Shelf Science, 162*, 7–21. https://doi.org/10.1016/j.ecss.2015.03.032

Harvey, M. E., Giddings, S. N., Stein, E. D., Crooks, J. A., Whitcraft, C., Gallien, T., & Elwany, H. (2020). Effects of Elevated Sea Levels and Waves on Southern California Estuaries During the 2015–2016 El Niño. *Estuaries and Coasts, 43*(2), 256–271. https://doi.org/10.1007/s12237-019-00676-1

Harvey, M. E., Giddings, S. N., Pawlak, G., & Crooks, J. A. (2023). Hydrodynamic Variability of an Intermittently Closed Estuary over Interannual, Seasonal, Fortnightly, and Tidal Timescales. *Estuaries and Coasts, 46*(1), 84–108. https://doi.org/10.1007/s12237-021-01014-0

Kelleghan, D. B., O'Callaghan, L., Huggard, F., Crowe, T. P., & Brooks, P. R. (2023). Using valve gape analysis to compare sensitivity of native Mytilus edulis to invasive Magallana gigas when exposed to heavy metal contamination. *Marine Environmental Research, 189*, Article 106043. https://doi.org/10.1016/j.marenvres.2023.106043

Kennish, M.J. (Ed.). (2004). *Estuarine research, monitoring, and resource protection*. CRC Press.

Largier, J. L. (2023). Recognizing Low-Inflow Estuaries as a Common Estuary Paradigm. *Estuaries and Coasts, 46*(8), 1949–1970. https://doi.org/10.1007/s12237-023-01271-1

Levin, L. A., Mendoza, G. F., Neira, C., Giddings, S. N., & Crooks, J. A. (2023). Consequences of Mouth Closure and Hypoxia-Induced State Changes in Low-Inflow Estuaries: Benthic Community and Trait-Based Response. *Estuaries and Coasts, 46*(8), 2128–2147. https://doi.org/10.1007/s12237-022-01132-3

Los Peñasquitos Lagoon Enhancement Plan. (2018). Los Peñasquitos Lagoon Foundation.

Marceau, F. (1909). Recherches sur la morphologie, l'histologie et la physiologie comparées de muscles adducteurs des mollusques acéphales Archives de zoologie experimentale et generale.

McSweeney, S. L., Kennedy, D. M., Rutherfurd, I. D., & Stout, J. C. (2017). Intermittently Closed/Open Lakes and Lagoons: Their global distribution and boundary conditions. *Geomorphology, 292*, 142–152. https://doi.org/10.1016/j.geomorph.2017.04.022

Meira, A., Carvalho, F., Castro, P., & Sousa, R. (2024). Applications of biosensors in non-native freshwater species: A systematic review. *NeoBiota, 96*, 211–236. https://doi.org/10.3897/neobiota.96.128038

Miller, L. P. (2022). Monitoring Bivalve Behavior and Physiology in the Laboratory and Field Using Open-Source Tools. *Integrative and Comparative Biology, 62*(4), 1096–1110. https://doi.org/10.1093/icb/icac046

Miller, L. P., & Dowd, W. W. (2017). Multimodal in situ datalogging quantifies inter-individual variation in thermal experience and persistent origin effects on gaping behavior among intertidal mussels (Mytilus californianus). *Journal of Experimental Biology, 220*(22), 4305–4319. https://doi.org/10.1242/jeb.164020

Mladenov, N., Biggs, T., Ford, K., Garcia, S., Yuan, Y., Grant, A., & Liden, D. (2024). Evaluation of real-time fluorescence sensors and benchtop fluorescence for tracking and predicting sewage contamination in the Tijuana River Estuary at the US-Mexico border. *Science of The Total Environment, 950*, Article 175137. https://doi.org/10.1016/j.scitotenv.2024.175137

Novoa, A., Talley, T. S., Talley, D. M., Crooks, J. A., & Reyns, N. B. (2016). Spatial and Temporal Examination of Bivalve Communities in Several Estuaries of Southern California and Northern Baja California. *MX. PLOS ONE, 11*(2), Article e0148220. https://doi.org/10.1371/journal.pone.0148220

Orescanin, M. M., & Scooler, J. (2018). Observations of episodic breaching and closure at an ephemeral river. *Continental Shelf Research, 166*, 77–82. https://doi.org/10.1016/j.csr.2018.07.003

Porter, E. T., & Breitburg, D. L. (2016). Eastern oyster, Crassostrea virginica, valve gape behavior under diel-cycling hypoxia. *Marine Biology, 163*(10), 218. https://doi.org/10.1007/s00227-016-2980-1

Pratt, J. (2014). *California Inlets: A Coastal Management "No Man's Land"* (Tech. Rep.). Surfrider Foundation.

Rasmussen, L.L., Carter, M.L., Flick, R.E., Hilbern, M., Fumo, J.T., Cornuelle, B.D., & McGowan, J.A. (2020). A century of southern california coastal ocean temperature measurements. *Journal of Geophysical Research: Oceans*, *125*(5), e2019JC015673. https://doi.org/10.1029/2019JC015673.

Ridlon, A. D., Marks, A., Zabin, C. J., Zacherl, D., Allen, B., Crooks, J., & Wasson, K. (2021). Conservation of Marine Foundation Species: Learning from Native Oyster Restoration from California to British Columbia. *Estuaries and Coasts, 44*(7), 1723–1743. https://doi.org/10.1007/s12237-021-00920-7

Roegner, G.C., Diefenderfer, H.L., Borde, A.B., Thom, R.M., Dawley, E.M., Whiting, A.H.. Johnson, G.E. (2008). *Protocols for Monitoring Habitat Restoration Projects in the Lower Columbia River and Estuary* (Tech. Rep. Nos. PNNL-15793, 927720).

Rouleau, T., Colgan, C., Adkins, J., Anthony, C., Patty, D., Lyons, S., & Stevens, H. (2021). The Economic Value of America s Estuaries: 2021 Report. Publications.

SANDAG (2025). San Diego LOSSAN Rail Realignment Project Final Value Analysis Study Report.

Skelton, Z.R., McCormick, L.R., Kwan, G.T., Lonthair, J., Neira, C., Clements, S.M., & Wegner, N.C. (2024). Organismal responses to deteriorating water quality during the historic 2020 red tide off Southern California. *Elementa: Science of the Anthropocene*, *12*(1), 00067. https://doi.org/10.1525/elementa.2023.00067.

Southern California Wetlands Recovery Project (2018). *Wetlands on the Edge: The Future of Southern California's Wetlands: Regional Strategy 2018* (Tech. Rep.). California State Coastal Conservancy.

Stacey, M. T., Burau, J. R., & Monismith, S. G. (2001). Creation of residual flows in a partially stratified estuary. *Journal of Geophysical Research: Oceans, 106*(C8), 17013–17037. https://doi.org/10.1029/2000JC000576

Sugihara, G. (1994). Nonlinear forecasting for the classification of natural time series. *Philosophical Transactions of the Royal Society of London. Series A: Physical and Engineering Sciences*. https://doi.org/10.1098/rsta.1994.0106

Sugihara, G., & May, R. M. (1990). Nonlinear forecasting as a way of distinguishing chaos from measurement error in time series. *Nature, 344*(6268), 734–741. https://doi.org/10.1038/344734a0

Sugihara, G., May, R., Ye, H., Hsieh, C., Deyle, E., Fogarty, M., & Munch, S. (2012). Detecting Causality in Complex Ecosystems. *Science, 338*(6106), 496–500. https://doi.org/10.1126/science.1227079

Tran, D., Fournier, E., Durrieu, G., & Massabuau, J.-C. (2004). Copper detection in the Asiatic clam Corbicula fluminea: Optimum valve closure response. *Aquatic Toxicology, 66*(3), 333–343. https://doi.org/10.1016/j.aquatox.2004.01.006

Tran, D., Fournier, E., Durrieu, G., & Massabuau, J.-C. (2007). Inorganic mercury detection by valve closure response in the freshwater clam Corbicula fluminea: Integration of time and water metal concentration changes. *Environmental Toxicology and Chemistry, 26*(7), 1545–1551. https://doi.org/10.1897/06-390R1.1

Tran, D., Haberkorn, H., Soudant, P., Ciret, P., & Massabuau, J.-C. (2010). Behavioral responses of Crassostrea gigas exposed to the harmful algae Alexandrium minutum. *Aquaculture, 298*(3), 338–345. https://doi.org/10.1016/j.aquaculture.2009.10.030

Tran, D., Nadau, A., Durrieu, G., Ciret, P., Parisot, J.-P., & Massabuau, J.-C. (2011). Field Chronobiology of a Molluscan Bivalve: How the Moon and Sun Cycles Interact to Drive Oyster Activity Rhythms. *Chronobiology International, 28*(4), 307–317. https://doi.org/10.3109/07420528.2011.565897

Uncles, R. J., Stephens, J. A., & Smith, R. E. (2002). The dependence of estuarine turbidity on tidal intrusion length, tidal range and residence time. *Continental Shelf Research, 22*(11), 1835–1856. https://doi.org/10.1016/S0278-4343(02)00041-9

Vereycken, J. E., & Aldridge, D. C. (2023). Bivalve molluscs as biosensors of water quality: State of the art and future directions. *Hydrobiologia, 850*(2), 231–256. https://doi.org/10.1007/s10750-022-05057-7

Walker, J. B., O'Connor, K., Wasson, K., Crain, C., Johnston, K. K., Ambrose, R. F., & Stein, E. D. (2025). Sentinel site networks as a mechanism to evaluate progress toward meeting restoration goals in altered and unaltered landscapes. *Restoration Ecology, 33*(5), Article e70062. https://doi.org/10.1111/rec.70062

Wallace, A. (2023). *Assessing the effectiveness of integrated multi-trophic aquaculture for growing west coast venus clams* (Doctoral dissertation. University of San Diego. https://doi.org/10.22371/02.2023.002.

Willmott, C. J. (1981). On the Validation of Models. *Physical Geography, 2*(2), 184–194. https://doi.org/10.1080/02723646.1981.10642213

Wilson, R., Reuter, P., & Wahl, M. (2005). Muscling in on mussels: New insights into bivalve behaviour using vertebrate remote-sensing technology. *Marine Biology, 147*(5), 1165–1172. https://doi.org/10.1007/s00227-005-0021-6